

**ENHANCED SENSITIVITY OF MICRO MECHANICAL CHEMICAL SENSORS
THROUGH STRUCTURAL VARIATION**

Justin Clay Harris
DOE ERULF
The Ohio State University
Oak Ridge National Laboratory
Oak Ridge, Tennessee 37831-8039

December 6, 2000

Prepared in partial fulfillment of the requirements of the Office of Science, DOE ERULF under the direction of Dr. Panos G. Datskos in the Engineering Technology Division at Oak Ridge National Laboratory.

Participant:

Signature

Research Advisor:

Signature

ABSTRACT

“Enhanced Sensitivity of Micro Mechanical Chemical Sensors through Structural Variation” Justin Clay Harris (The Ohio State University, Marion, Ohio 43302-5695) Panos G. Datskos (Oak Ridge National Laboratory, Oak Ridge, Tennessee 37831-8039).

Chemical detection devices are very effective; however, their bulkiness makes them undesirable for portable applications. The next generation of chemical detectors is microscopic mechanical devices capable of measuring trace amounts of chemical vapor within the environment. The chemicals do not react directly with the detector, instead intermolecular forces cause chemicals to adhere to the surface. This surface adhesion of the chemical creates surface stress on the detectors leading to measurable movement. Modifications to the structural design of these microstructures have resulted in signal enhancement to over seven hundred percent.

Research Category

ERULF: Physics, Chemistry, and Engineering

School Author Attends: The Ohio State University
DOE National Laboratory Attended: Oak Ridge National Laboratory

Mentor's Name: Dr. Panos G. Datskos
Phone: 865-574-6205
e-mail: pgd@ornl.gov

Author's Name: Justin Clay Harris
Mailing Address: 833 Wyandot Road
City/State/Zip: Bucyrus OH 44820
Phone: 419-562-0812
e-mail Address: harris.594@osu.edu

Is this being submitted for publication?: Yes
Doe Program: ERULF

Table of Contents

Abstract	ii
Introduction	1 – 4
Experimental Setup	4 – 6
Sensor Fabrication	6 – 8
Procedure	8 – 10
Results	10
Discussion and Conclusions	10 – 11
Acknowledgements	11 – 12
References	13
Figures	14 - 21

Introduction

The field of Micro Electro Mechanical Systems (MEMS) is multi-disciplinary, encompassing nearly all aspects of science. MEMS are a derivative of Micro Electronic Systems (MES), used to miniaturize electrical circuitry. Electronic sensors and mechanical actuators are the main emphasis in the diverse world of MEMS. For example, MEMS devices small enough to be placed on the head of a pen, but powerful enough to sense a change in acceleration and trigger an airbag explosion, saving lives. Millions of pivoting mirrors controlled by a computer system are now being used in some top of the line high definition televisions. These televisions are much lighter and thinner than the traditional picture tube style. The benefits of these micro electro mechanical systems may be easy to see, but development of it is more difficult than first glances may show.

Differences between our world and the micro world cause scientists, working on this level, to live in a sort of “dream world.” Thinking about objects that are barely seen by the best eyes and working with imperceptible forces can give even the best scholars trouble. For example, in the macroscopic world, ignored intermolecular forces are not of major consequence and gravitational forces are the focus. In the microscopic world however, just the opposite is true. Intermolecular forces cause dust, sometimes half the size of the device, to stick to surfaces making them difficult to work with. These forces also cause devices to “stick” to nearby surfaces, leaving movement nearly impossible. Although micro-sized devices sound extremely difficult to work with, many benefits accompany the solvable difficulties. For example, MEMS have a small enough mass that even large acceleration changes result in very little momentum change. This allows these

microstructures to withstand hundreds of times gravitational acceleration. They are therefore virtually indestructible when placed away from physical contact. This among many other differences resulted in increased reliability, accuracy, and speed as well as decreased size, expense, and power consumption.

One group of MEMS electronic sensors currently in development is chemical detectors. These MEMS sensors could help to monitor trace amounts of chemical exposure to any number of various vapors. Individuals using various pin-on detectors could work close to hazardous chemicals without the worry of coming in contact with problematic amounts of vapor. These detectors could warn when various vapors are present within the surrounding air, working as a sort of artificial nose. They could “sniff” out drugs or explosives for police, and be more cost effective than training and maintaining a squadron of dogs. A perfect application of this technology would be for detection of chemical warfare agents, protecting soldiers from death or disorder.

Chemical adsorption onto surfaces, currently under research at Oak Ridge National Laboratories (ORNL), is a phenomenon that could be the basis for micro chemical detection devices. Using this method, chemicals adsorb onto the surface of a cantilevered beam acting as the detector. This cantilevered beam is a small bi-material structure, called a micro cantilever, that preferentially adsorbs chemical on one side, resulting in cantilever bending. “The micro cantilever bending results from unbalanced adsorption-induced differential surface stress.” (Datskos et al., 1999) In the past, researchers were only capable of working with macro-sized objects, where differential surface stress from chemical adsorption would not have caused measurable movement.

Now that microscopic cantilevers are being mass-produced, it makes adsorption a viable chemical detection method.

The chemical adsorption technique has already been tested and shown to work by Datskos et al in 1999. (Datskos et al., 1999) In his method, a triangular micro cantilever typically used by an atomic force microscope (AFM) became the detector. This detector was primarily silicon nitride with a thin uniform layer of gold one side. Because 2-mercaptoethanol preferentially adsorbs to gold, a stress occurred and the cantilever bent a measurable amount.

The ORNL researchers' original goal was to prove that the chemical adsorption technique worked. Now that scientists accept chemical adsorption as a possible basis for chemical detectors, optimizing signal strength must occur to develop a useful device. Cantilevers, designed for use by the atomic force microscope and purchased from Park Scientific Instruments, became the primary focus of device optimization. These cantilevers, illustrated in Figure 1, were chosen do to their availability, low cost, and miniscule size tolerances. Cantilever C, the starting point for development, has the most sensitivity to chemicals, because it is much longer than the other cantilevers. Earlier attempts at increasing sensitivity have included cuts made by focused ion beam milling (FIB) to effectively triple to quintuple the effective leg length and thinning of the legs with the FIB. Figure 2 shows a cantilever with an effectively tripled leg length.

This study uses cantilever C in Figure 1 in an attempt to optimize the chemical absorption signal through geometrical alterations. Chemical adsorbed primarily to one surface of the cantilever makes it deflect. A laser and a quad cell position detector measured the cantilever deflection. These experimental results, as well as results from

previous alterations, will lead researchers to develop a minute, accurate, and trustworthy chemical sensor.

Experimental Setup

The experimental setup consists of a cantilever used as the sensor, the gas flow system discussed later, and the devices used to measure cantilever deflection, shown in Figure 3. To measure cantilever deflection, a laser reflects off the head of a cantilever into a quad cell detector. This sounds simple, but is a bit more complicated. A 5 mW diode laser with a circular aperture is focused down using a lens into a 5 μm pinhole. After the beam comes through the pinhole, it is collimated with another lens and then focused onto the cantilever head with yet a third lens. Placed in a certain position, the cantilever reflects the laser beam away from the previous lens and into another lens. This last lens focused the reflected laser beam to a mirror and into the quad cell detector.

“The quad cell detector is a four-channel position-sensing detector capable of sub-nanometer resolution.” (Datskos et al. 1997) Because of the way the cantilever is mounted, horizontal movement is measured. The detection part of the quad cell uses a $\frac{1}{2}$ inch diameter silicon chip that changes voltage output as light intensity changes. Since the chip is divided into four sections, see Figure 4, it can easily detect movement. As shown in Equation 1, channels 1 and 3 are added together as well as 2 and 4. The results are subtracted and then divided by a normalizing sum of 1, 2, 3, and 4.

$$V_h = \frac{(V_1 + V_3) - (V_2 + V_4)}{\sum_{i=1}^4 V_i} \quad (1)$$

where V_h is the horizontal voltage
 V_1 is voltage from quadrant one
 V_2 is voltage from quadrant two
 V_3 is voltage from quadrant three
 V_4 is voltage from quadrant four

Initially the laser beam is centered, but as the cantilever bends horizontally, the quad cell electronically computes the above formula and outputs a signal. This signal is received in an oscilloscope and a lock in amplifier. In this experiment, the lock in amplifier simply records data. The oscilloscope is required to initially center the laser beam accurately, and as a total voltage meter. By keeping the total voltage at 6.8 volts, well within the quad cell detectors optimum range, normalization of resulting data was not necessary.

To understand the way the detector works and to make any geometrical modifications to a cantilever, knowledge of structure is important. The cantilever used in all experiments is the triangular cantilever C in Figure 1, purchased from Park Scientific Instruments. This cantilever has an overall length of 320 μm , a width of 22 μm , and a thickness of 0.6 μm . The cantilever is a bi-material made of silicon nitride with a 60 nm coating of gold on one side. This bi-material cantilever allows preferential adsorption of the chemical causing surface tension and the bending effect.

The final part of the experimental setup is the gas flow system shown in Figures 6, 7, and 8. Nitrogen flows into the gas flow system through a mass flow controller. Since chemical concentrations depend upon this controller, calibration was necessary and the procedure went as follows. A graduated cylinder filled with water was inverted into a beaker of water. Then the nitrogen was allowed to bubble up into the graduated cylinder for one minute. The amount of gas, which escaped for each mass controller setting, was recorded and formulated into a calibration curve shown in Figure 5.

The flow system is designed for three different parts of the experiment. First, nitrogen must be drawn into the syringe pump. Second, chemical vapor is pumped straight to the waste line while nitrogen is flowed over the cantilever in an enclosed vessel. Finally, chemical vapor is pumped into the flow of nitrogen, where it mixes with nitrogen and flows to the cantilever. These are shown in Figures 6, 7, and 8 respectively. Nitrogen is represented by blue, chemical liquid and vapor by yellow, and the mixture by green. Valve positions are green and red, which stand for open and closed respectively. As the most important part of the experimental setup, the micro cantilever must also be discussed.

Sensor Fabrication

As mentioned earlier, the purchased cantilever used in the experiment came from Park Scientific Instruments, see Figure 1. By making geometrical variations to cantilever C with a focused ion beam mill (FIB), different sensors were fabricated. Four different structures were used: un-modified, notched, grooved, and re-grooved. All geometrical modifications were cuts into the cantilever legs attempting to make them more sensitive.

Cuts were made on the side of which the cantilever bends toward. This would decrease the need to compress that side as the cantilever bends. To find the direction in which bending occurred, a heat source was brought near to the cantilever. The signal from heat showed the cantilever bending in one direction. When the same cantilever was later exposed to chemical, the cantilever signal shows it bending in the opposite direction. To realize which direction the cantilever bends after the addition of chemical vapor, the material properties must be studied. By previous studies of materials, it is known that gold expands more than silicon nitride when heated. From this, it is safe to deduce that the cantilever is bending toward the silicon nitride when heated, and as described above it bends opposite to that when chemical is added. For this reason, cuts were always made into the gold side of the cantilever. A description of the exact modifications to each cantilever is as follows.

For the control group of the experiment, the chip, shown in Figure 1, from Park Scientific Instruments was used. Cantilever C would have the greatest response because of its larger leg surface area and overall length. A decision was made to make it the cantilever of choice for the control group. It became the starting point for all geometrical modifications.

Before notches can be made, the sputter rate must be measured. To do this, a 10 μm by 10 μm hole was milled by the FIB through the 0.6 μm silicon nitride and gold of another cantilever. The end point was visually detected. By using Equation 2.1, the size of the hole, the time measured to mill the hole, and the current setting on the FIB, the sputter rate was calculated.

The first of the modifications to cantilevers were notches cut into the legs. Into each leg, five notches, see Figure 9, were made on the gold side of the cantilever with a focused ion beam mill (FIB). These notches were 25 μm by 25 μm by 0.3 μm deep. To calculate a specific amount of time for milling the notches Equation 2.2, a rearrangement of Equation 2.1, was used.

$$V = t \times I \times Sr \quad (2.1)$$

$$t = \frac{V}{I \times Sr} \quad (2.2)$$

where V is volume (μm^3)
 t is time (s)
 I is current (nA)
 Sr is sputter rate $\left(\frac{\text{nm}^3}{\text{nC}} \right)$

For the third and fourth cantilevers, thin grooves were milled into the legs. These grooves were 25 μm by 0.1 μm by 0.3 μm deep. Again, equation 2.2 was used, and it was verified by milling an equivalent line completely through a neighboring cantilever. The third, grooved cantilever, had five grooves milled into each leg, see Figure 10, and the fourth was the same cantilever with five more grooves milled into each leg in between the first, see Figure 11.

Procedure

Before testing any cantilevers for their response, trial runs were completed with only nitrogen flowing. Because nitrogen flowed in from outside of the temperature controlled room and from the syringe pump, located within the room, a variance was inevitable. Remember that these cantilevers are a bi-material; any slight temperature change causes a slight bending. All testing occurred when trial runs showed a near flat temperature induced signal between the outdoor nitrogen flow and the indoor nitrogen flow, see Figure 12. Since some tests were up to ninety minutes in length, during which a significant outdoor temperature change could occur, a simple subtraction between the trial and the test signals became impractical. This would also have been the largest reason for any experimental error within the data.

For each cantilever, four tests and the above trials were completed. For the first and second test, the cantilever was exposed to ethanol vapor forced out of a vial and carried by nitrogen at 0.5 mL/min. This nitrogen/ethanol mixture was turned on and off before it mixed with a stream of nitrogen flowing at 2 mL/min. The final stream of nitrogen carrying ethanol reaches the cantilever, adsorbs, and causes it to bend. Two tests were carried out to show the repeatability. The other two tests were completed with the same procedure, except with aniline and at a primary flow of 1 mL/min. This flowed into the 2 mL/min stream and was carried to the cantilever. Again, two tests were completed to show repeatability. Different times were needed for adsorption to take place, but there was always a ten minute time period, at the beginning, where only the secondary nitrogen flowed at 2 mL/min. This allowed the setup to show its stability. In all graphs, the sudden drop shows where the chemical was turned on and the sudden rise

indicates the time at which the chemical was turned off. Figures 13 and 14 show this phenomenon, but they also show the ease at determining whether the chemical is aniline or ethanol. It obviously is not a precise match among all chemicals, but it shows that a chemical is in the cantilever's environment.

Results

As a baseline for all tests, an unmodified cantilever was tested. Upon the completion of this test, a 50 mV deflection was noticed for both aniline and nitrogen. Within the surrounding noise, this signal was barely detectable, see Figure 15. The cantilever with the five notches soared to a 350 mV signal, a 700% increase from the base line. This alteration did not increase the ambient noise level either, therefore, the signal to noise ratio increased by 700% as well. For the cantilever with five grooves, the signal reached 170 mV, a 240% increase from the baseline. When five more grooves were added, the signal dropped 30 mV to a signal of 140 mV, this left only a 180% increase from the baseline. See Figure 16 for cantilever comparison.

Discussion and Conclusions

From data collected during this project, it is worth noting that the notched cantilever had a response seven times that of the unmodified cantilever. This is most likely due to the decrease in tension while bending. However, tension while bending is not the only variable in making cantilevers that are more sensitive.

The cantilever with five grooves responded better than the cantilever with ten grooves. At first glance this does not make sense, but with more careful thought it

becomes quite apparent. The mechanism that originally caused the cantilever to bend is the preferential adsorption to the silicon nitride side. Remember that the milling was done on the gold side, thus exposing the underlying silicon nitride for chemical adsorption. In turn, this adsorption causes the cantilever to push against the preferred bending. As a result, the cantilever bends toward the gold side, but with less deflection than the cantilever with five grooves. There will definitely be a point of maximum deflection, depending upon the surface area of silicon nitride exposed.

According to this very concept, it is safe to say that a gold coating could increase the signal even more. An atomically thin layer of gold could be placed upon those surface areas exposed by the milling process. This layer would stop the adsorption in those areas, again lessening the forces against the desired motion. Since the surface area exposed on the notched cantilever is nearly half of the desired side's surface area, the cantilever deflection should double after a gold coating.

Signal enhancement by geometrical alteration was the primary goal of this project. The data collected shows that this goal has been met but needs to be explored in much further detail.

Acknowledgements

I thank the United States Department of Energy for this opportunity to participate in this undergraduate research program. My thanks go to my mentor Dr. Panos G. Datskos, and the entire MEMS and NEMS group in the Engineering Technology Division at Oak Ridge National Laboratory. In addition, a special thanks goes out to Matt Martin and Shawn Goedeke for giving me helpful guidance throughout this project.

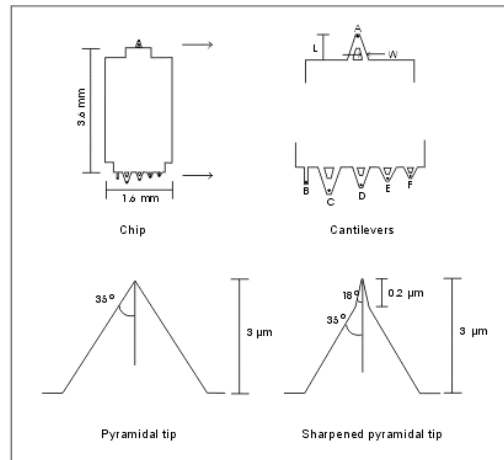
I must thank my parents for the powerful strength they have given me to accomplish many goals throughout my life. My girlfriend, Karen Dolan, deserves a tremendous thank you for giving me the encouragement to push through the rough times and make yet another dream a reality.

The research described in this paper was performed within the Engineering Technology Division at the Oak Ridge National Laboratory. It was sponsored by the United States Department of Energy under the Energy Research Undergraduate Laboratory Fellowship program (ERULF).

References

- Datskos, Panos, I. Sauers. *Detection of 2-mercptoethanol using gold-coated micromachined cantilevers*. **Sensors and Actuators. B** 61. p. 75-82. 1999.
- Datskos, Panos, S. Rajic, I. Datskou, C. M. Egert. *Infrared Microcalorimetric Spectroscopy Using Uncooled Thermal Detetors*. **SPIE**. vol. 3118. p. 280-287. 1997.
- Martin, Matt. *Microscopic Thermal Detector Optimization Through Material and Geometric Selection*. Masters Thesis in preparation. 2000

Figures



Typical Mechanical Characteristics

Cantilever type	A - triangular	B - rectangular	C - triangular	D - triangular	E - triangular	F - triangular
Standard mode of operation	Contact					
Cantilever length	180 μm	200 μm	320 μm	220 μm	140 μm	85 μm
Cantilever width	18 μm	20 μm	22 μm	22 μm	18 μm	18 μm
Cantilever thickness	0.6 μm	0.6 μm	0.6 μm	0.6 μm	0.6 μm	0.6 μm
Force Constant	0.05 N/m	0.02 N/m	0.01 N/m	0.03 N/m	0.10 N/m	0.50 N/m
Resonant Frequency	22 kHz	15 kHz	7 kHz	15 kHz	38 kHz	120 kHz

Figure 1. 1 Existing cantilever design (Microlevers 2000)

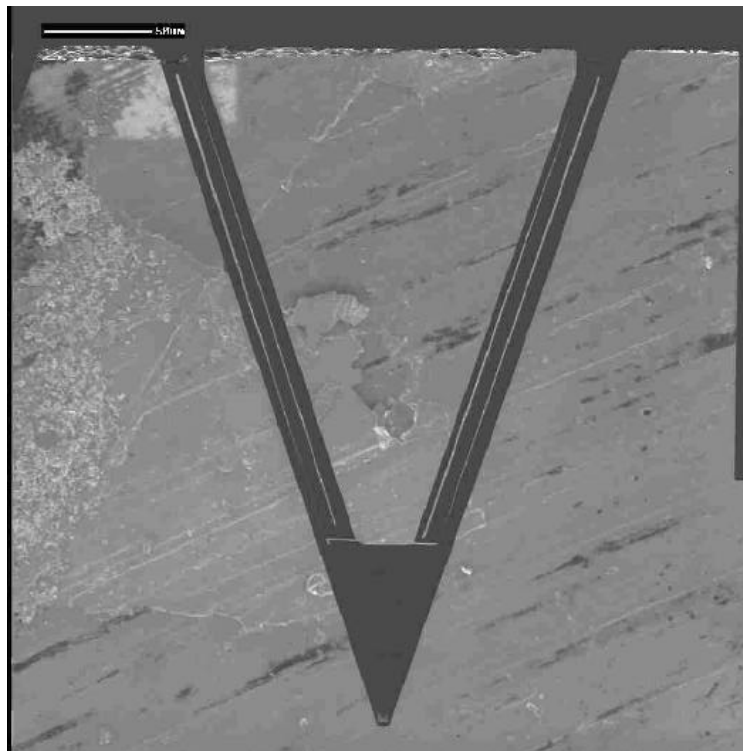


Figure 2 Geometrically altered cantilever resulting in triple effective leg length

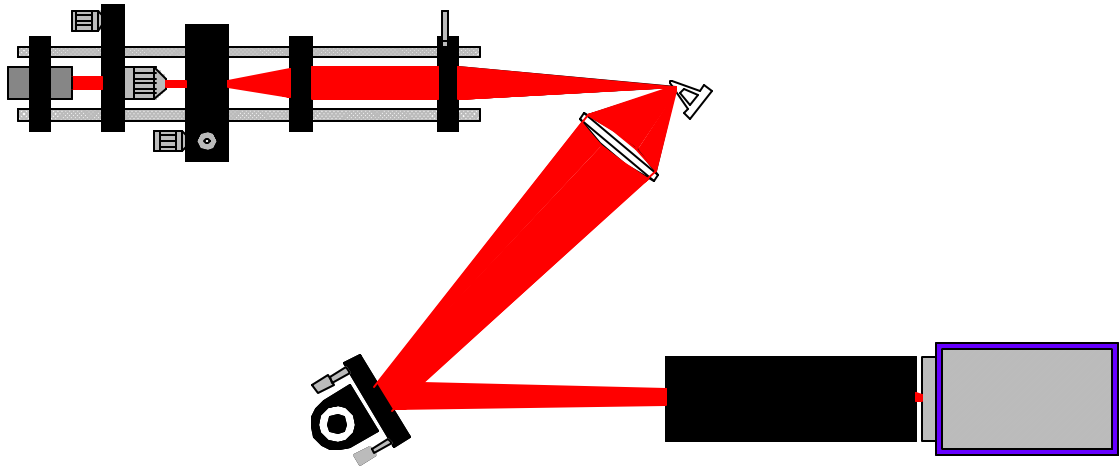


Figure 3 Optical setup

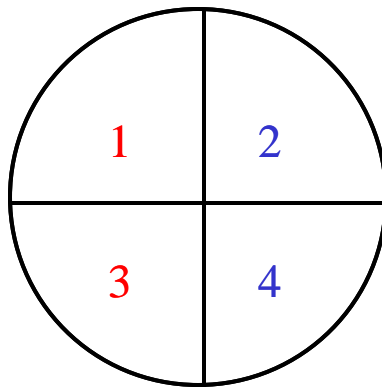


Figure 4 Quad cell detector face (Martin 2000)

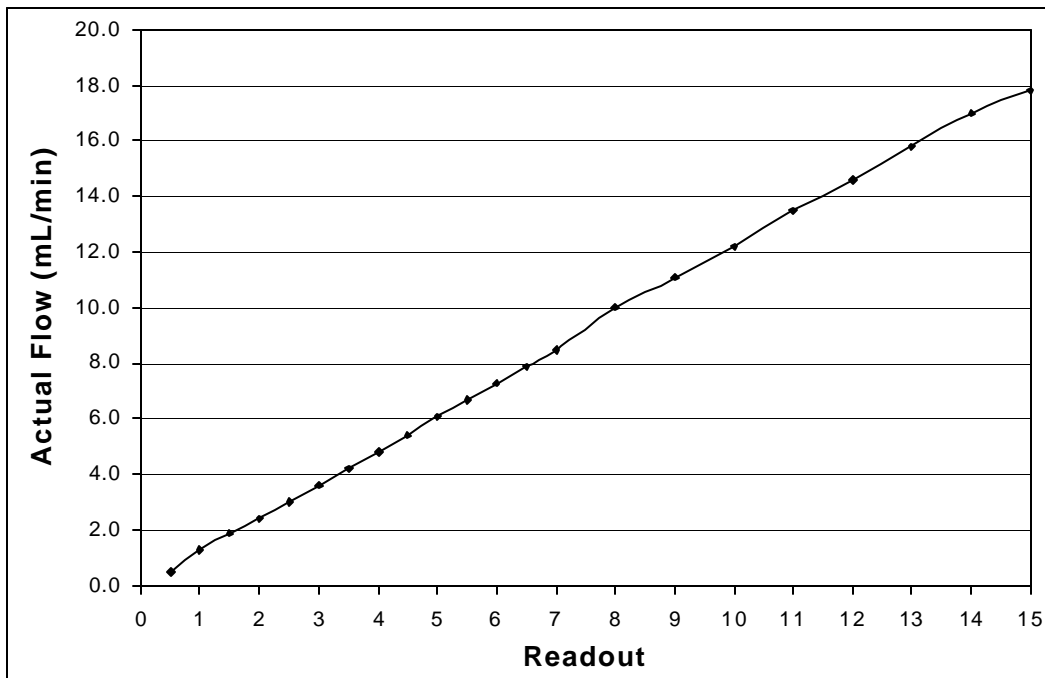


Figure 5 Calibration curve of mass flow meter

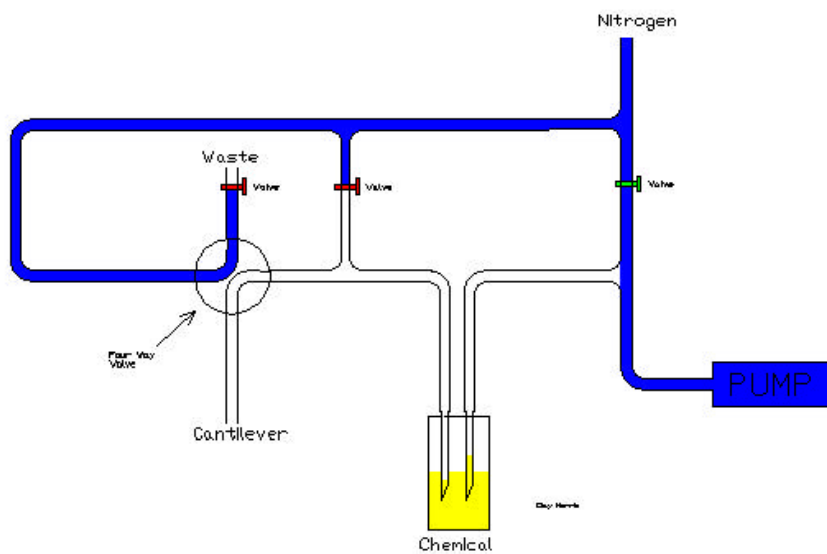


Figure 6 Draw nitrogen into syringe pump

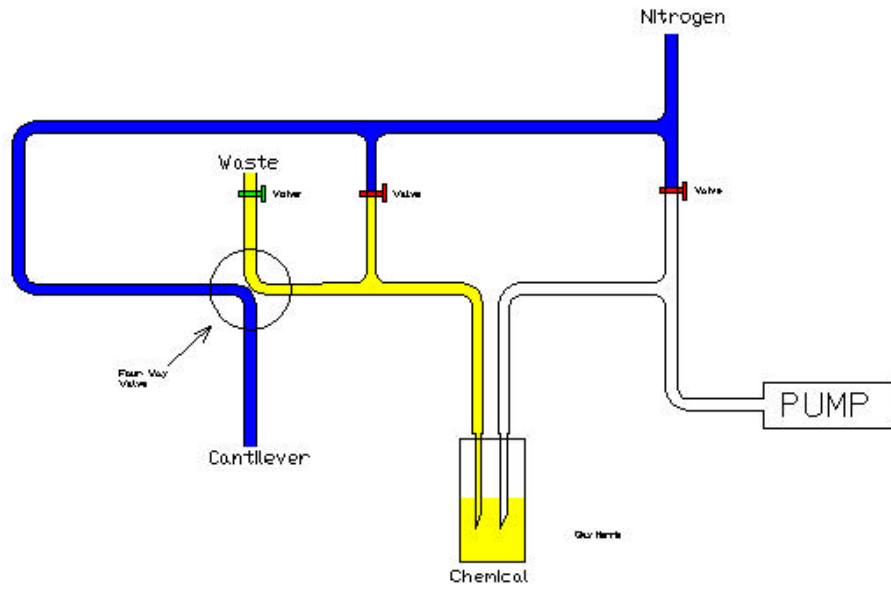


Figure 7 Flowing nitrogen to cantilever

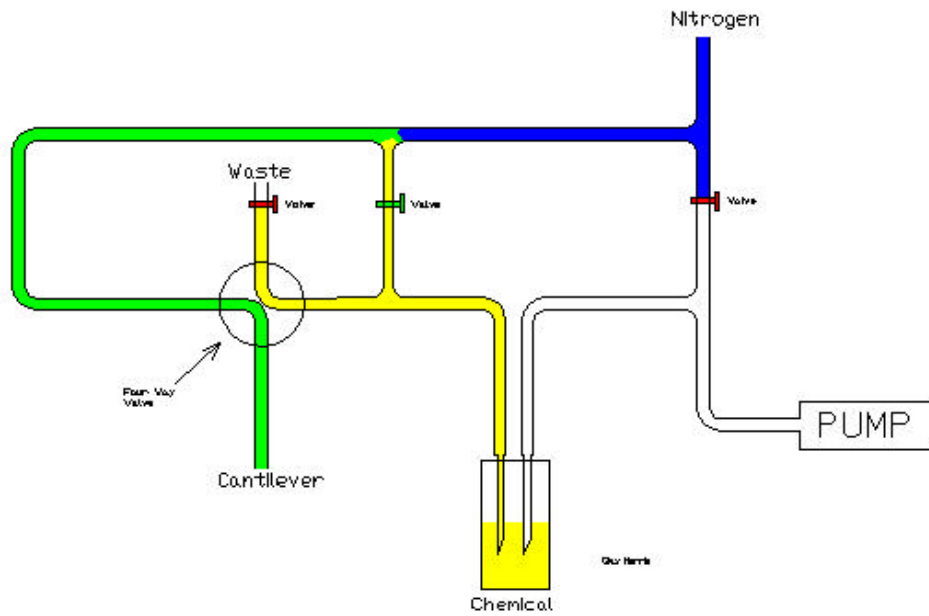


Figure 8 Flowing nitrogen / chemical mixture to cantilever



Figure 9 Notched cantilever

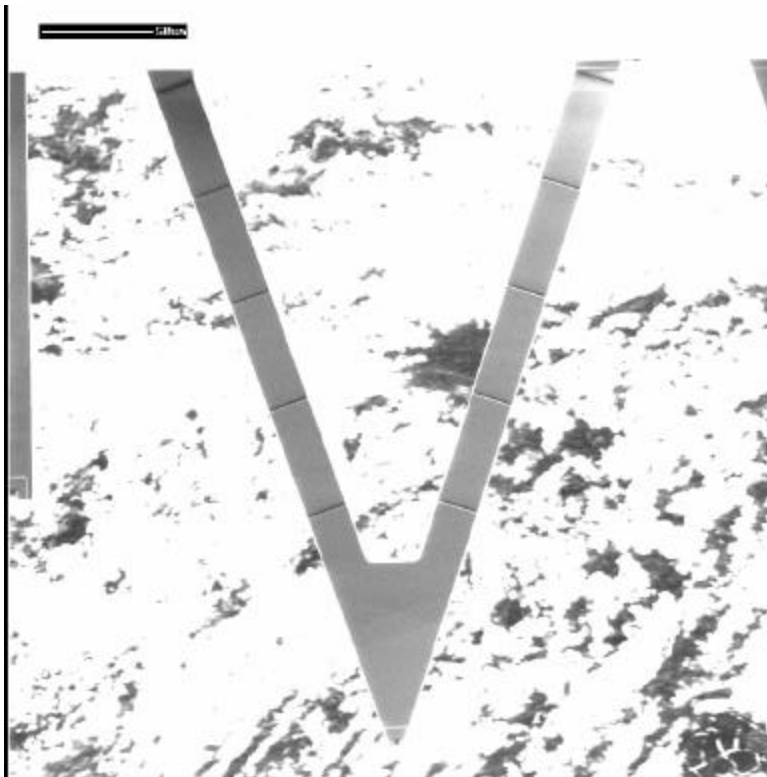


Figure 10 Grooved cantilever

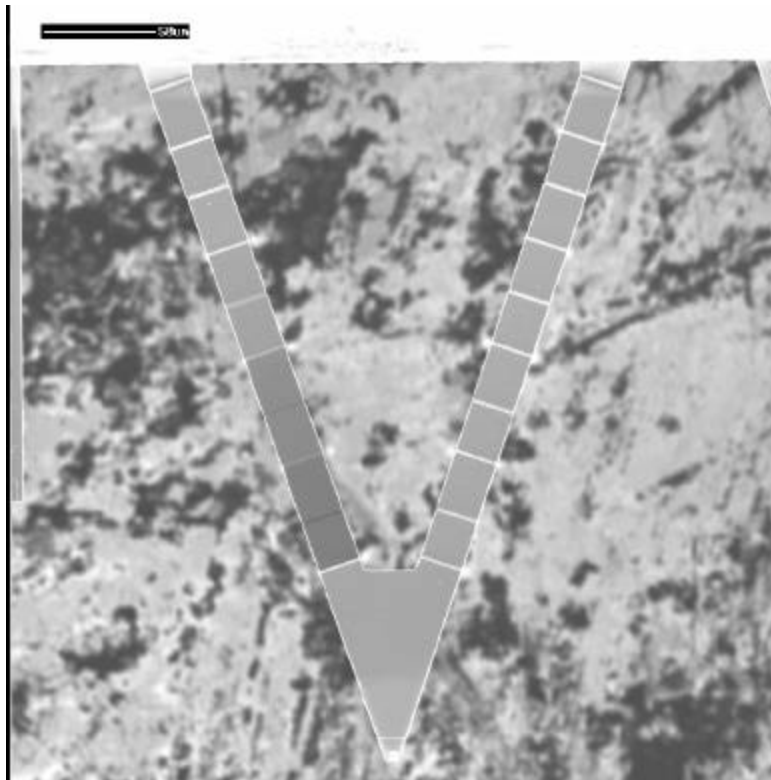


Figure 11 Re-grooved cantilever

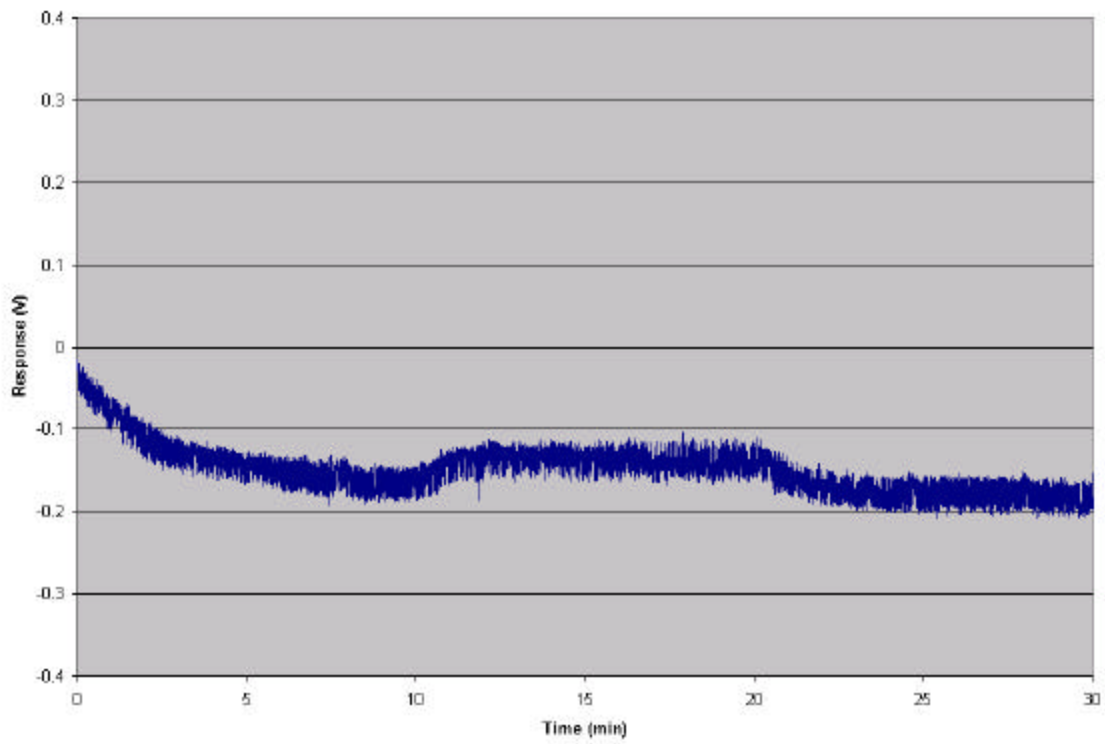


Figure 12 Signal from nitrogen temperature variation

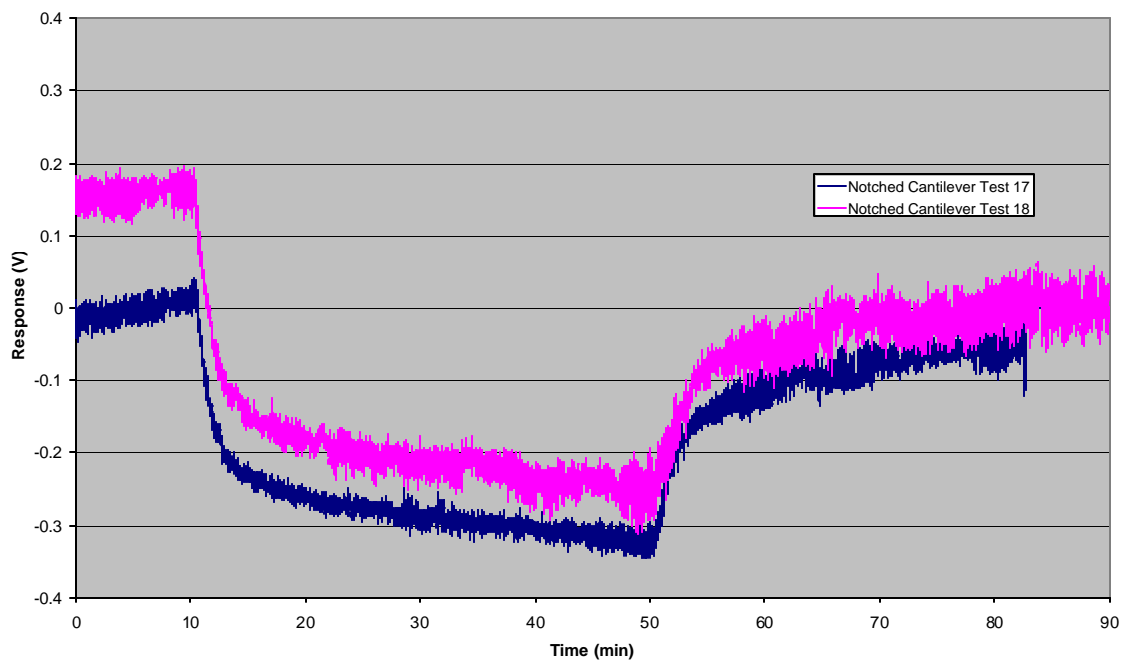


Figure 13 Response from ethanol with notched cantilever

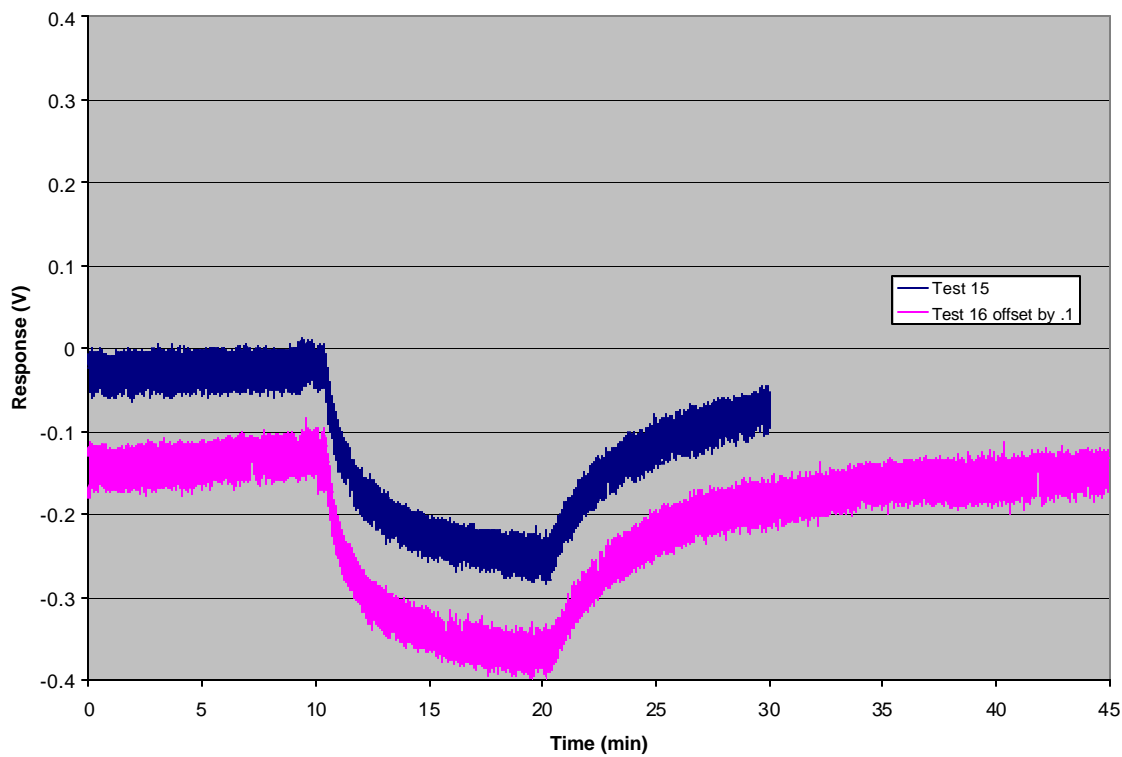


Figure 14 Response from aniline with notched cantilever

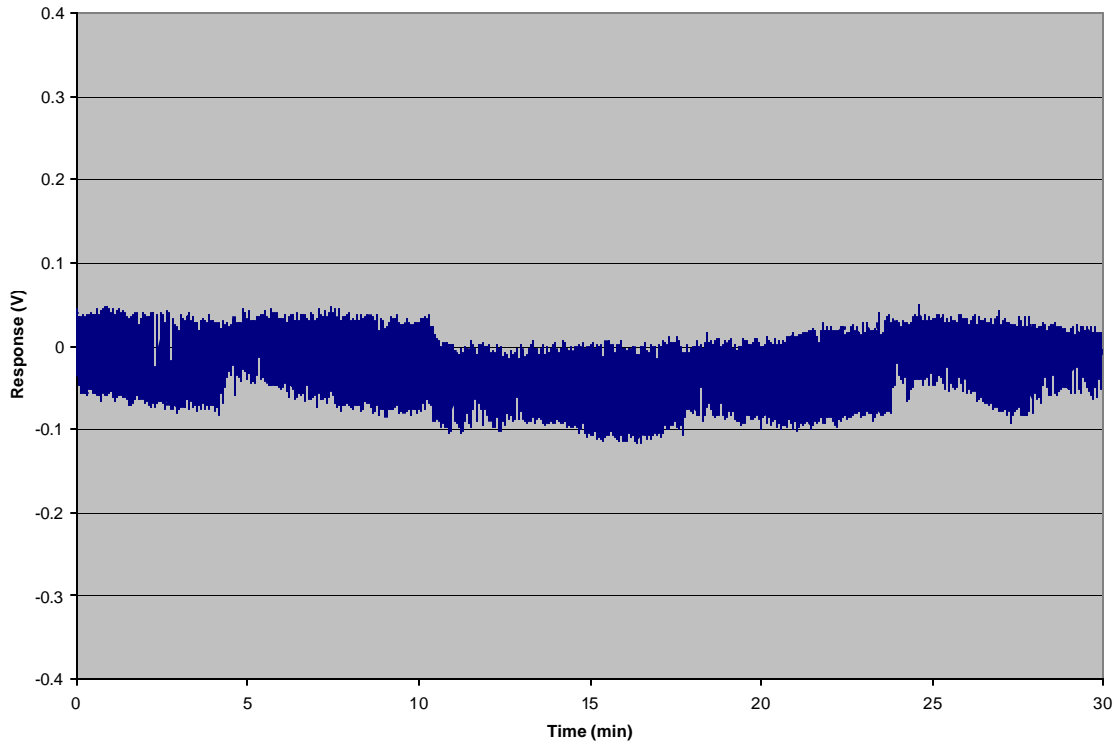


Figure 15 Noise and signal from an unmodified cantilever

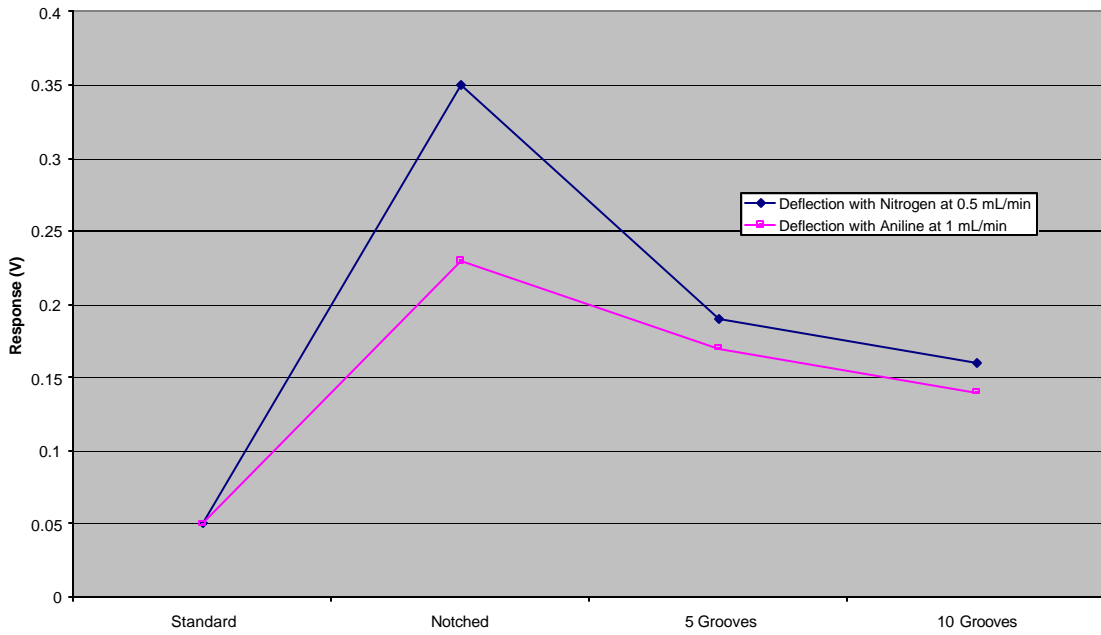


Figure 16 Comparison of cantilever responses